



## UTILIZATION OF MAGNETIC SIGNATURE OF AUTOMOTIVE TIRE FOR EXPLOITATIONAL WEAR ASSESSMENT

Sebastian BROL<sup>1</sup> , Jan WARCZEK<sup>2,\*</sup> 

<sup>1</sup> Politechnika Opolska, Wydział Mechaniczny

<sup>2</sup> Politechnika Śląska, Wydział Transportu i Inżynierii Lotniczej

\* Corresponding author, e-mail: [s.brol@po.edu.pl](mailto:s.brol@po.edu.pl)

### Abstract

Summary The use of tires is limited, on the one hand, by their geometric wear, which is interpreted by vehicle users as the tread height, on the other hand, as a result of aging processes. There is an intrinsic magnetic field around the tire. This specific feature of the tire can be interpreted as the magnetic pattern of the tire. The aim of the research was to determine the influence of operation on the distribution of magnetic induction around the tire. The tests were carried out on new tires and after a specific operational mileage. The obtained results in the form of spatial images of the distribution of the magnetic field force lines of new tires and after a specific operational mileage allowed to visualize the differences in their technical condition, which were not possible to observe using other research methods.

Keywords: tire, magnetism, wear

### List of Symbols/Acronyms

- $\mathbf{B}$  – induction vector which consists of so many projection as used in utilized magnetic sensor design (in this investigations 3)
- $B_k$  – particular projection of  $\mathbf{B}$ , i.e.  $B_k$  can be either:  $B_x$ ,  $B_y$ , or  $B_z$ ;
- $h$  – distance from magnetic sensor to steel belt;
- $i$  – index of specific sample in circumferential magnetic profile;
- $k$  – projection name: x, y or z.;
- $MDq$  – parameter of magnetic circumferential profile given by (1) and explained in figure 3
- $N$  – number of samples in circumferential magnetic profile;
- $w$  – angle of rotation;

### 1. INTRODUCTION

Tires used in automobiles, which an example is shown in Figure 1. Are build using parts of different properties. Some elements of tire (tread, arm, side) are used to provide flexibility and assumed damping and the other (steel belt/belts, cords) are used to assure directional stiffness and form when under specific loads [27, 28].

A wide range of materials are used to manufacture tire and tire components. One of distinguished element is so called steel belt. It consists of steel elements, which reminds simple wires, but often they are twisted by two or even more to add rigidity. The name “steel belt” is confusing because it is not a belt in common sense but rather

some layers of steel wires of diameter varying from 0.1mm up to 0.5mm. In every layer the single wires or twisted wires are arranged parallel and embedded in rubber. There are at least two sheets lying one above the top of other. The wires in one sheet are aligned at some specific angle to the other. If looking from above it looks like mesh, which buckles the tire.

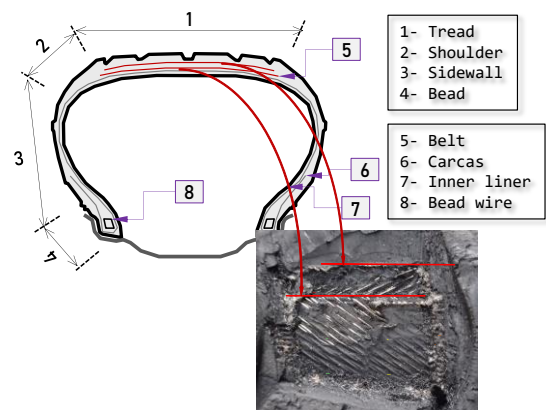


Fig. 1. Crossection of tire and top-view of a layers in steel-belt structure

The steel belt is strong and therefore it is placed beneath of the tread. During wheels rotation the steel mesh deforms similarly (but not the same) as tread. The deflection of the tire during car's movement depends on many factors: mainly on static and dynamic load and tires radial stiffness which is related to pumping pressure [19, 1, 16].

Combining three facts: (1) that the steel belt is beneath the tread, (2) deflects with it as the complete wheel rotates (3) the deflection may not be the same (but similar) because of the rubber thickness between belt and tread, can lead to thesis, that tire wear can be judged by steel belt's properties.

One of such property can be the tire's magnetic signature. It comes from both rotation in Earth's magnetic field and from Villari effect as the belt flexes and changes orientation. The Earth's induction varies from  $25\mu\text{T}$  to  $60\mu\text{T}$  [20, 25, 14]. The rotation frequency of the wheel can vary from almost 0 Hz to even up to 50Hz in case of sport cars [8,22] but the belt flexing in tire-ground contact area can achieve even 7 times more. Combined influence can change the steel belt magnetic field value [17] and its signature [22]. The changes in magnetic field signature can be very fast and dramatic judging by magnetic profiles and surfaces [17, 18, 10, 25].

There are some measurement techniques which can be applied. For example Stankowski [9], Jacobs et al. [10] and Kawase et al. [12, 13], used hand held devices and also instruments combined with fixtures to handle and rotate the wheel and measure magnetic profile acquired in time domain [7, 23]. Other method is proposed by Brol et al. in [2] (Fig 2).

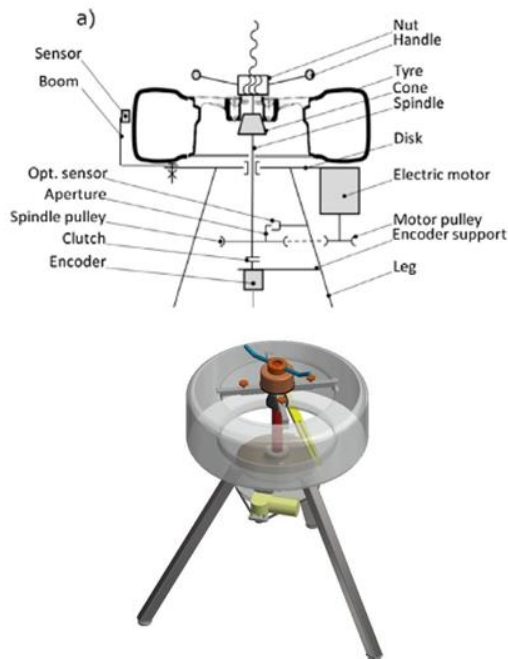


Fig. 2. Device for magnetic profiles measurement and with ability to perform scan of magnetic surface over steel-belt [2]

The measurement is made in angle of rotation domain and allows to measure circumferential and cross profiles as well as magnetic plane scan over tread and steel belt which is located beneath tire's tread. Different sensors were used for this measure described also in [24, 29]. The rebuild and improved measurement system will be discussed in next sections of this article.

## 1. INSTRUMENTS AND METHODS

### 1.1. The sensor

3-axis anisotropic magnetoresistive HMC5883L sensor is utilized [9,27]. It is selected because of selectable measurement range, low price, and data transmission using I2C bus. The maximum sampling frequency is 160Hz. The sensor's resolution and accuracy is  $0.48 \cdot 10^{-7}\text{T}$  and  $2 \cdot 10^{-7}\text{T}$  accordingly.

### 1.1. Measurement method

For this investigations magnetic plane scans (2D) were selected as method of tire's magnetic field measurement over tread (and steel belt), which is depicted in Figure 3. As it also can be seen this method allows simultaneously to measure cross and circumferential profiles of vector  $B$  as well [21]

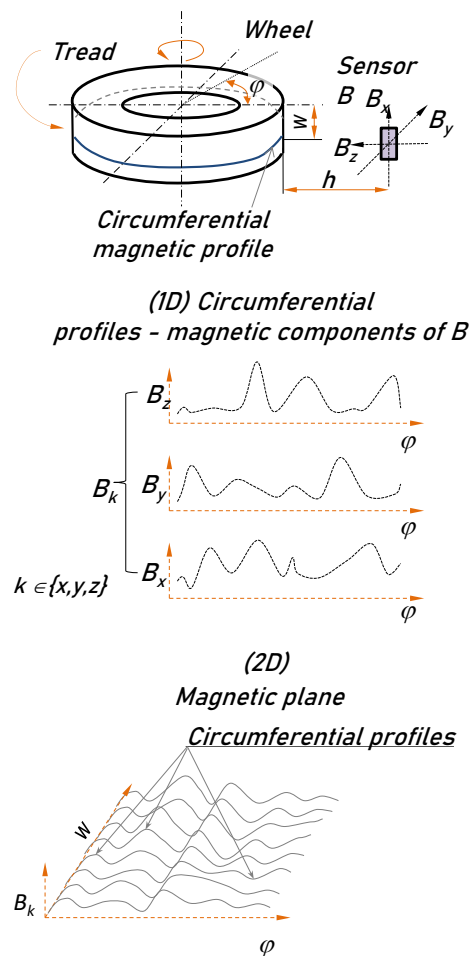


Fig. 3. Schematic of magnetic circumferential profile measurement (1D) and magnetic plane measurement (2D)

To be precise, the  $B$  vector can consist of many projections of  $B$ . This depends on sensor design, specifically in number of measurement axis (for example 3 of them:  $B_x$ ,  $B_y$ ,  $B_z$ ). Therefore the circumferential magnetic profile can consists of one of four profiles, namely  $B_x$ ,  $B_y$ ,  $B_z$  and  $|B|$ .

The plane measurement method is the (2D) spatial scan over thread's surface. The scan is

usually made on area defined by circumference of tire and (usually) width of tread. The result of such measurement is so called magnetic surface and it consists of finite number of circumferential profiles measured at selected tread width. Measurement of B in angle domain using the device new design (Figure 4) provide desired repeatability of measurement of circumferential profiles [6]. Moreover angular velocity can't be too high because of centrifugal force which can cause inaccuracies induced by vibrations [3, 4, 11, 15, 26] therefore a rotational speed controller is utilized.

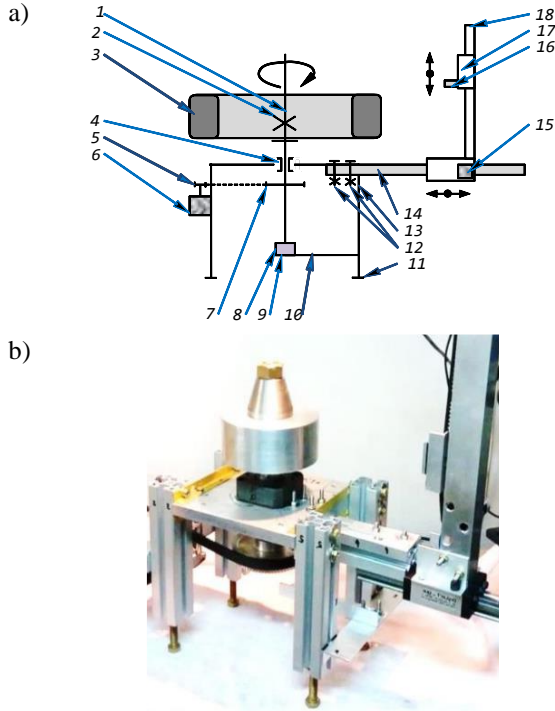


Fig. 4. Original measurement device schematic (a). 1—main shaft, 2—fastening nut, 3—wheel, 4—bearing, 5,7—sprockets, 6—electric motor, 8—encoder, 9—encoder's base plate, 10—arm, 11—foot, 12—locking screws, 13—leg, 14—guide, 15—electric motor, 16—sensor, 17—slide, 18—pol. (b) Original photo of measuring device.

The final parameters of complete measurement device is provided in Table 1.

### 3. THE EXPERIMENT

#### 3.1. The object

There were 4 wheels by the same vendor exanimated mounted on steel rims. The exploitation parameter were as depicted on Figure 5.

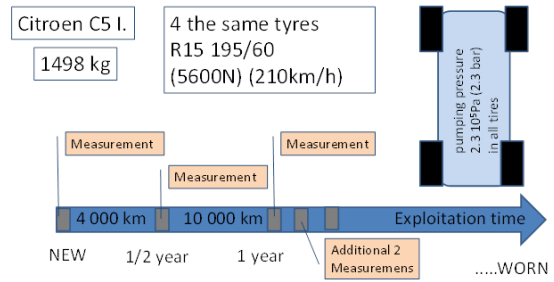


Fig. 5. Properties of object of investigations and measurements time and distance (please refer Fig. 8 for precise distance of additional measurements)

There were winter tires used. This is because usually this kind of tires has no twisted wires in steel belt mesh. Therefore a much faster reaction to tread wear was expected. Moreover winter tyre's rubber wears faster when exploited on summer rough roads. And this is rather important if time of experiment (very long) is taken into account. All wheels were exploited on the same position in a car, and its alignment in relation to hub were kept the same during experimentation.

Table 1. Measuring device mechanical characteristics

Parameter	Range	Comment
Rims	12'' to 30''	Light alloys, steel
Rotational speed of spindle	0.104 to 0.314 rad/s	0.5 ÷ 1.5 rpm, 0.25 rpm increment
Max angular resolution	Up to 4096 samples per 0.087° rot. ±0.0015 rad	selectable
Circumferential resolution	0.25 to 0.6 mm	Related to wheel's free radius during measurement
Type of magnetic sensor	3D (3 Cartesian proj. of B)	Anisotropic, magnetoresist. HMC 5883L
Sensor dimensions	3.0mmx3.0mmx0.9mmLxWxH	
Range and resolution of magnetic sensor	From ±1.5·10 <sup>-4</sup> T to ±8.1·10 <sup>-4</sup> T, 12bit	
Greatest std. dev. of 4095 samples measured at stop	±1.9·10 <sup>-7</sup> T	Max of std. dev. Meas. on x,y, and z axis
Distance to thread surface, h	10 to 300mm	Additional fixture can be used
Width of tread (w) at measurement	0 to 220mm	Additional fixture can be used

### 3.2. Experiment

The car was undergo normal exploitation in European circumstances. Daily distance was about 14km-25km in urban and sub-urban conditions. One fourth of the distance was made with constant speed about 90km/h and rest of it at 50km/h. During experiment long trips were also made, which contribute into total mileage. The pressure were monitored every week, and restored if needed always in cool tires.

### 3.3. Analysis course

In this investigations only change of magnetic signature of the front wheels were shown. This is because the front wheels are more loaded statically and also undergo much more torsional and side forces than the rear's. Moreover because of not exchanging the wheels every season (that means front with rear) the wear of the front wheels is more distinctive [5].

During analysis the magnetic signatures of magnetic planes (2D) of  $B_x$ ,  $B_y$ ,  $B_z$  and resultant  $|B|$  of  $\mathbf{B}$  vector were analysed.

## 4. THE RESULTS

The first observation made was fact, that this particular tires show walls of local maxima for every component and resultant  $B$  remaining from new to wear tires as can be seen on Figure 6.

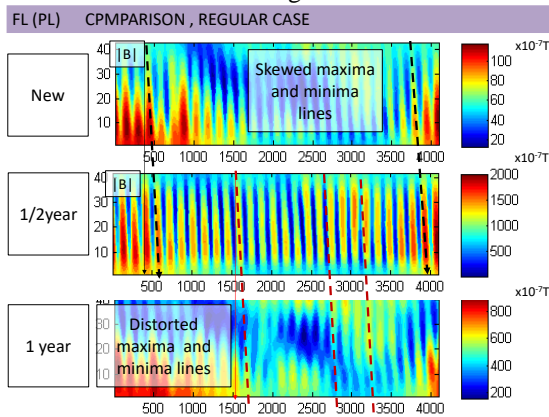


Fig. 5. Magnetic signatures of  $B_x$  components for measured planes (2D) of front left (FR) wheel.

This means that all  $B$  components are in phase and can be considered as remaining after production process. Surprisingly the maxima walls are not perpendicular to direction of rotation but skewed at some angle. And this angle changes during exploitation especially at edges of the tire's steel belt after 1 yr of exploitation. This is the first premise that magnetic signature changes with time of exploitation. More harder is to explain this phenomena because it can be caused at least by two factors lateral forces created by toe in wheel aligning or by tread wear which de facto is non-uniform and is about 10% grater at outer sides of front wheels. This is usual situation for front drive cars (like this

one used in investigations) with McPerson's strut suspension in which toe-in is preferred.

The change in magnetic field amplitude distribution is more obvious if considering  $B_x$  component on Figure 7. Through 0.5 yr the changes are little and subtle, but after 1 yr the changes are more distinctive. The  $B_x$  component is perpendicular do rotation direction therefore conclusion can be drawn out that this kind of changes can be an effect of lateral forces affecting the wheel. Moreover the changes are concentrated on outer side of wheel where also the wear is by 10% greater.

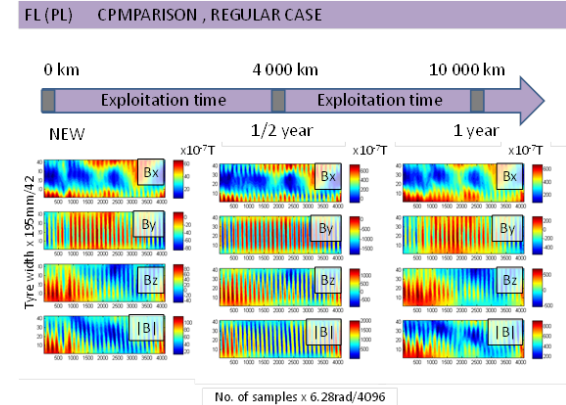


Fig. 7. Magnetic signatures of  $B$  components and resultant for measured planes (2D) of front left (FR) wheel.

It is worth noting (even if it is out of scope of this paper), that the rear wheels show almost the same changes in magnetic signature with exception that there is no side where the amplitude changes are concentrated.

There is also an exception in investigation. After one year of exploitation an singularity appeared in magnetic signature of the front left wheel. It has typical shape of magnetic field change ( $B_x$  and  $B_y$  components) and maximum for  $B_z$  component (marked areas on Figure 8). It can be a sign of increased stresses acting on belt structure or sign of it delamination. We are more convinced to the second option but at the time both possibilities have the same probability.

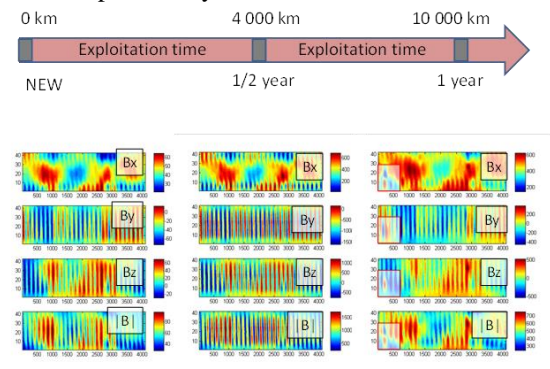


Fig. 8. Magnetic signatures of  $B$  components and resultant for measured planes (2D) of front left (FR) wheel.

Since amplitude distribution analysis shows already that there is no relation with time of exploitation then the spatial properties seems to be 'sensitive' to it therefore in the next part of investigations parameters of magnetic profiles. Especially the spatial ones and the hybrid were used as defined in [2].

The MDq parameter given by (1) appeared to be sensitive to time of exploitation and to distance travelled (mileage), but there is a catch: this is a hybrid parameter, so both spatial and amplitude properties influences their value.

$$MDq = \frac{1}{2\pi N} \sum_{i=2}^N |B_{k,i} - B_{k,i-1}| \quad (1)$$

Therefore it was decided to normalize the profile first to new range from 0..1 and calculate the MDq after normalization. The results are shown on Figure 9a and 9b.

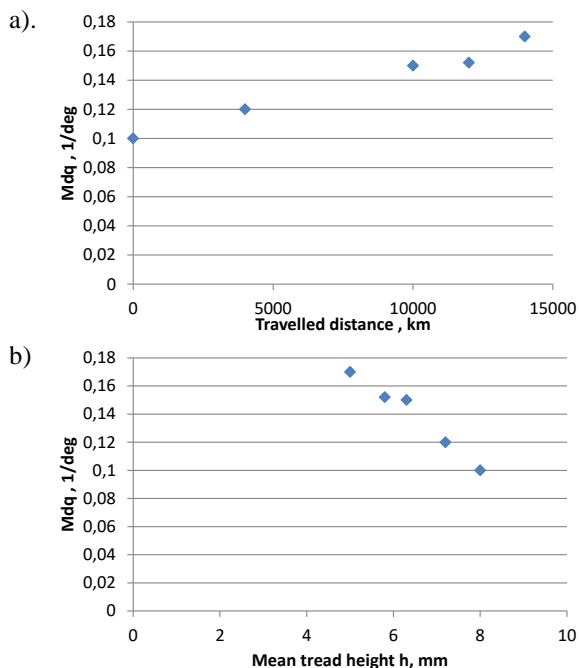


Fig. 9. MDq parameter vs mean tread height (a) and MDq parameter vs travelled distance (b) for FR wheel for middle circumferential profiles (from 20-th to 22-th) which corresponds to tire width from 92mm to 102mm

It must be clearly noted that not all profiles in magnetic signature satisfying this regularity. This is only true for front right and for both rear wheels. The reason for exclusion of from left wheel is the singularity shown in Figure 8, which influences the results.

## CONCLUSIONS

The following conclusions can be drawn out the investigations:

1. In this investigations the new tyres from one producer have the similar magnetic field pattern with distinctive walls of extrema almost perpendicular to rotation direction. The

amplitudes of all B components are relatively low and can be considered as remaining of production process.

2. After half year of exploitation the tyres magnetization increases by factor of ca 10, and after 1 year it decrease by factor of ca. 2 but the pattern shape changes a little in that time. After 1 year the magnetization in almost all measured planes reduces by factor of 2 for every component in comparison to the half year exploitation state.
3. At this moment only one profile one circumferential profile parameter parameter correlates with time of exploitation and travelled distance. It is the MDq parameter evaluated on normalized Bx component of circumferential profiles in middle of surface scan (i.e. from 92mm to 102mm of tire width)

**Author contributions:** *research concept and design, S.B., J.W.; Collection and/or assembly of data, S.B.; Data analysis and interpretation, S.B., J.W.; Writing the article, S.B.; Critical revision of the article, S.B., J.W.; Final approval of the article, S.B.*

**Declaration of competing interest:** *The authors declare that they have no known competing financial interests or personal relationships that could have appeared to influence the work reported in this paper.*

## REFERENCES

1. Andrzejewski R. Dynamika Pneumatycznego koła jezdneho. WNT Warszawa, 2010 (in Polish).
2. Brol S, Szegda A. (2018). Magnetism of automotive wheels with pneumatic radial tires. Measurement. 2018;126:37-45. <https://doi.org/10.1016/j.measurement.2018.05.034>.
3. Brol S. Progress in application of portable accelerometer based measurement systems in powertrain performance testing performed on road. SAE Technical Paper 2013-01-1433, 2013. <https://doi.org/10.4271/2013-01-1433>.
4. Brol S; Mamala J. Application of Spectral and Wavelet Analysis in Power Train System Diagnostic. SAE Technical Paper 2010-01-0250, 2010. <https://doi.org/10.4271/2010-01-0250>.
5. Caban J; Drożdźiel P, Barta D, Liščák Š. Vehicle tire pressure monitoring systems. Diagnostyka 2014; 15(3):11-1426.
6. Díaz-Rodríguez ID, Han S; Bhattacharyya S. Analytical Design of PID Controllers. Springer 2019.
7. Gontarz S, Radkowski S. Impact of different factors on relationship between stress and eigenmagnetic field in steel specimen. IEEE Transactions on Magnetics 2012;48(3).
8. Halgamuge MN, Abeyrathne CD, Mendis P. Measurement and Analysis of Electromagnetic fields from tams, trains and hybrid cars. Radiation Protection Dosimetry. 2000;141(3):255-268. <https://doi.org/10.1093/rpd/ncq168>.
9. Grzesik W, Brol S. Identification of surface generation mechanisms based on process feed-back and decomposition of feed marks. Advanced Materials Research. 2011;223:505-513.

- <https://doi.org/10.4028/www.scientific.net/AMR.223.505>.
10. Jacobs WL, Dietrich F.M, Feero WE, Brecher A. Assessment of magnetic fields produced by spinning steel belted radial tires. EPRI/DOE Annual Review of Research on Biological Effects of Electric and Magnetic Fields from the Generation. 1998.
  11. Jantos J, Brol S; Mamala J. Problems in assessing road vehicle driveability parameters determined with the aid of accelerometer. SAE Technical Paper 2007-01-1473. 2007. <https://doi.org/10.4271/2007-01-1473>.
  12. Kawase M, Tazaki S. Method for detecting the magnetic field of a tire. US 6404182 B1, 2001.
  13. Kawase M, Tazaki S, Kaneko H, Sato H, Urayama, N. Method and apparatus for detecting tire revolution using magnetic field, US 6246226 B1, 2002.
  14. LeGoff A, Lacoume, J-L, Blanpain R, Dauve' S, Serviere C. Automobile wheel clearance estimation using magnetism. Mechanical Systems and Signal Processing. 2012;26:315–319. <https://doi.org/10.1016/j.ymssp.2011.07.011>.
  15. Mamala J, Brol S, Jantos J. The estimation of the engine power with use of an accelerometer. SAE Technical Paper 2010-01-0929. 2010. <https://doi.org/10.4271/2010-01-0929>.
  16. Miliken, W, Miliken D. Race Car vehicle Dynamics 1995. New York: J. Wiley & Sons.
  17. Milham S, Hatfield JB, Tell R. Magnetic Fields From Steel-Belted Radial Tires: Implications for Epidemiologic Studies. Bioelectromagnetics 1998.
  18. Milham S, Hatfield JB, Tell R. Magnetic fields from steel-belted radial tires implications for epidemiologic studies. Bioelectromagnetics. 1999; 20:440-445.
  19. Mitschke M. Dynamika samochodu. T. 2 Drgania. WKiŁ, Warszawa. 1989.
  20. Ptitsyna NG, Ponzetto A, Kopytenko YuA; Ismagilov VS, Korobeinikov AG. Electric Vehicle Magnetic Fields and Their Biological Relevance, Journal of Scientific Research & Reports. 2014;3(13):1753-1770.
  21. Praznowski K, Brol S, Augustynowicz A. Identification of static unbalance wheel of passenger car carried out on a road. Solid State Phenomena. 2013;214:48-57.
  22. Stankowski S; Kessi A, Be'cheiraz O, Meier-Engel, K, Meier M. Low frequency magnetic fields induced by car tire magnetization. Health Physics. 2006. <https://doi.org/10.1097/01.HP.0000174526.10639.ff>.
  23. Szegda A, Brol S. Measurement device of magnetic flux density of tire. Proceedings of Institute of Vehicle 2017;12:121-128.
  24. Szulim P, Mączak J, Rokicki K, Lubikowski K. Application of low-cost magnetic field and acceleration sensors in diagnostics of large-size structures. Diagnostyka. 2013;14(4):43-49.
  25. Vedholm K. Personal exposure resulting from low-frequency electromagnetic fields in automobiles. Thesis Gothenburg 1996.
  26. Więclawski K, Mączak J, Szczurowski K. Electric current as a source of information about control parameters of indirect injection fuel injector. Eksploatacja i Niezawodność. 2020;22(3):449-454. <https://doi.org/10.17531/ein.2020.3.7>.
  27. [www.yokohama.com/global/product/tire/learn/knowledge/nomenclature/](http://www.yokohama.com/global/product/tire/learn/knowledge/nomenclature/). 2020.
  28. <https://dadbloguk.com/wp-content/uploads/2017/10/Tyre-cross-section.jpg>. 2020.

29. <http://www.farnell.com/datasheets/1683374.pdf>. 2020.

Received 2022-09-12

Accepted 2022-11-03

Available online 2022-11-17



Dr hab. inż. **Sebastian BROL**, prof. PO – zajmuje się: zagadnieniami związanymi z modelowaniem dynamiki pojazdów samochodowych, diagnostyką techniczną, badaniami symulacyjnymi i eksploatacyjnymi, przepływem energii w układach napędowych oraz mechatroniką a także zastosowaniem falek i fraktali w obszarach aktywności naukowej.

Autor lub współautor kilku książek i monografii oraz wielu artykułów w czasopiśmie krajowych i zagranicznych. Wykonawca kilku projektów badawczych i wdrożeniowych zrealizowanych we współpracy z przemysłem.

Członek Polskiego Towarzystwa Diagnostyki Technicznej oraz Polskiego Towarzystwa Naukowego Silników Spalinowych.



Dr hab. inż. **Jan WARCZEK** - zainteresowania badawcze: zagadnienia związane z modelowaniem dynamiki zawieszonych pojazdów samochodowych, diagnostyka techniczna, analiza sygnałów WA, badania symulacyjne i eksploatacyjne tłumienia drgań, przepływ energii w układach mechanicznych, metody badań nieniszczących.

Autor lub współautor 4 publikacji książkowych oraz wielu artykułów w czasopiśmie krajowych i zagranicznych. Kierownik lub wykonawca kilku projektów badawczych i wdrożeniowych we współpracy z podmiotami przemysłowymi.

Członek Polskiego Towarzystwa Diagnostyki Technicznej oraz Polskiego Naukowo- Technicznego Towarzystwa Eksploatacji. Członek Komisji Transportu PAN o. Katowice.